PAPER

Check for updates

Pyrolysis of sweet lemon (*Citrus limetta*) waste: effect of zeolite β, ammonium on kinetics and bio-oil yield

Faisal Muhammad,[a] Jan Nisar, ID *[a] Ghulam Ali,[a] Farooq Anwar,*[bc] Wan Azlina Wan Abdul Karim Ghani,[d] Ahsan Sharif[e] and Ejaz Ahmed[e]

This study aims to explore the potential of citrus waste for valuable products. A special pyrolysis chamber was used to produce bio-oil through thermo-catalytic pyrolysis of sweet lemon (*Citrus limetta*) waste with a zeolite β, ammonium catalyst. The kinetic parameters were derived from thermogravimetric data using the Kissinger equation. The activation energy and frequency factor values for hemicellulose, cellulose, and lignin were determined to be 83.14, 108.08, and 124.71 kJ mol^{-1} and 6.3×10^4, 9.4×10^6, 2.6×10^9 min^{-1}, respectively. GC-MS analysis of the bio-oil revealed a variety of fuel-range hydrocarbons. Additionally, the biochar generated from non-catalytic and catalytic pyrolysis was compared, exhibiting different surface characteristics, as evident by scanning electron and transmission electron microscopy images. Our findings indicated that zeolite β, ammonium served as an effective catalyst by reducing the activation energy and lowering the temperature required for maximum degradation during pyrolysis, ultimately yielding a diverse array of useful products from citrus waste compared to the non-catalyzed reaction. Based on the fuel properties, it was concluded that the bio-oil, if slightly upgraded using the appropriate techniques, has a promising future as a green fuel.

1. Introduction

The rapid increase in population and shift in lifestyle have significantly heightened the demand for energy.[1] Fossil fuels have traditionally been the major source of energy[2]; however, industrialization and technological advancement have led to their accelerated consumption, resulting in alarming depletion rates.[3] Furthermore, their combustion contributes to global warming, adversely affecting the environment.[4] In light of dwindling fossil fuel supplies and their potential role in climate change, researchers and the global community are actively seeking environmentally friendly alternatives.[5–7] The urgent need to address fossil fuel shortages and their impact on climate change has

become a global concern, prompting researchers and international organizations to explore sustainable energy sources. The United Nations Climate Panel has targeted 50% to 80% reduction in greenhouse gas emission by 2050, emphasizing the importance of switching to renewable energy sources from non-renewable ones. As a result, renewable energy is increasingly being recognized as essential for sustainable development and environmental preservation.[8]

Biofuels are gaining significant recognition as a green fuel due to their ability to emit fewer harmful gases, such as NOx and SOx, compared to fossil fuels. In recent years, considerable research has been conducted on the potential utilization of biomass to produce biofuels because of its affordability and environmental sustainability.[9,10] Biomass serves as a promising source for mitigating harmful emissions, alongside other renewable sources.[11,12] The utilization of biomass as a sustainable energy source is compelling due to its positive impact on the environment and eco-friendliness. One of the notable advantages of biomass conversion is its ability to be compressed into a reduced volume, which facilitates easy storage, transportation, and long-term preservation without decomposition.[13] Moreover, lifecycle analysis indicates that biofuels, particularly biodiesel, can substantially reduce greenhouse gas (GHG) emissions compared to petroleum diesel.

Citrus fruits are widely cultivated in many parts of the world and play a significant role in human nutrition.[14] Roughly half

[a] *National Centre of Excellence in Physical Chemistry, University of Peshawar, Peshawar 25120, Pakistan. E-mail: jan_nisar@uop.edu.pk, pashkalawati@gmail.com*
[b] *Department of Food Science, Faculty of Food Science and Technology, Universiti Putra Malaysia, 43400 UPM Serdang, Selangor, Malaysia. E-mail: farooq@upm.edu.my, fqanwar@yahoo.com*
[c] *Institute of Chemistry, University of Sargodha, Sargodha-40100, Pakistan*
[d] *Sustainable Process Engineering Research Centre (SPERC), Department of Chemical and Environmental Engineering, Universiti Putra Malaysia, 43400 Serdang, Selangor, Malaysia*
[e] *School of Chemistry, University of the Punjab, New Campus, Lahore 54590, Pakistan*

of the wet fruit mass consists of citrus waste, which is produced by the fruit processing industry after juice extraction. This waste primarily consists of peel and pulp.[15] Citrus peel and pulp, as lignocellulosic materials, predominantly consist of fibers and essential oils. These components can be extracted and utilized in various industries, including medicinal and cosmetic. Moreover, citrus fruit waste (peels and pulp) mainly consists of hemicellulose, cellulose and lignin, which can be utilized as a valuable raw biomass for producing a variety of bio-chemicals and bio-fuels.[16]

Worldwide, significant volumes of biomass waste are produced, including leftovers from the harvest and processing of fruit crops, which have significant potential to be transformed into biofuel. However, there is still a dearth of studies focusing on the pyrolysis kinetics of *Citrus limetta* waste over zeolite β, ammonium. Hence, the key objective of this work was to evaluate the efficacy of zeolite β, ammonium as a catalyst for the decomposition of citrus waste into biofuel. The kinetic parameters of the reaction associated with this conversion were also determined. Additionally, it was determined how various parameters such as catalyst, temperature, and pyrolysis time affect the pyrolysis of *Citrus limetta* waste.

2. Experimental

2.1. Materials and methods

Juice-extracted sweet lemon (*Citrus limetta*) waste (properly authenticated by a botanist) was sourced from a juice shop in Faisalabad city, Punjab, Pakistan. The collected biomass was shade-dried for 21 days, ground into a fine powder using a grinder, sieved to the desired mesh size, and stored in a sealed bag for further analyses. The elemental characteristics and structure of raw biomass were examined using energy dispersive X-ray spectroscopy and SEM. To improve the quality of oil produced, zeolite β, ammonium was selected as the catalyst among several commercial options.

2.2. Thermogravimetric analysis of citrus waste and kinetic study

TGA of citrus waste loaded with zeolite β, ammonium was conducted on a PerkinElmer Q500 at different temperature programme rates (15, 20, 25, and 30 °C min^{-1}). The obtained TGA results were then used to determine the E_a and A-factor through the following Kissinger equation.[17]

$$\ln\left[\frac{\beta}{T_m^2}\right] = \ln\left(\frac{A.R}{E_a}\right) - \frac{E_a}{RT_m} \qquad (1)$$

In eqn (1), T_m stands for maximum degradation temperature, β refers to temperature programme rate, and R denotes gas constant. E_a and A-factor were computed from the slopes and intercepts of $\ln \beta/T_m^2$ *vs.* $1000/T_m$ plots, respectively.

2.3. Pyrolysis experiments and products characterization

In order to minimize heat loss in an inert atmosphere, citrus wastes loaded with zeolite β, ammonium catalyst were pyrolyzed in a salt bath (containing mixture of $NaNO_2$, $NaNO_3$ and KNO_3) packed in a stainless-steel vessel enclosed in another vessel with insulating material. The pyrolysis process is schematically diagrammed in Fig. 1.[18,19] For each experiment, 5 grams of citrus waste was placed in the reaction vessel and secured within the salt bath. The resulting vapours were directed through a condenser, where they were condensed into a liquid fraction. A GC-MS instrument (GC7890B MS5977B Agilent) was used to chemically characterize the recovered bio-oil. The analysis was carried out through an HP-5 capillary column. Helium gas was employed as the carrier gas and the injector was kept in the split mode at 25 °C. The column was kept at 40 °C in an oven for 15 min, then increased to 160 °C at 10 °C min^{-1} and held for 8 min. After that, it was heated to 290 °C at a rate of 10 °C per minute and kept there for one minute. The analysis took a total of 24 minutes and the identities of peaks were made through the NIST library. Moreover, the identity of the components in
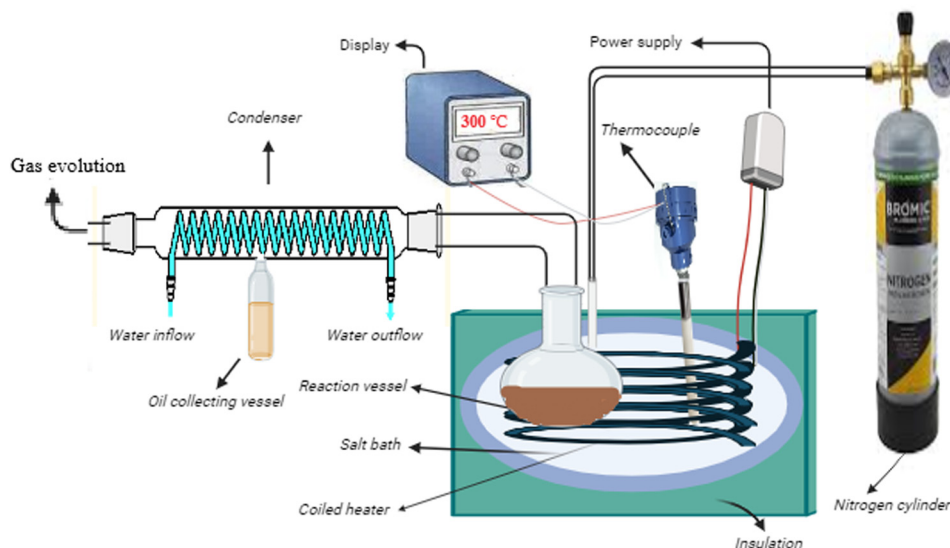

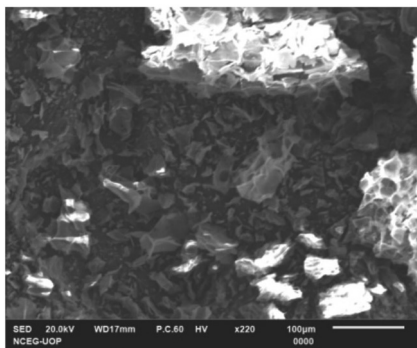Fig. 1 Schematic of the pyrolysis setup.

Fig. 2 SEM image of *Citrus limetta* waste.

the bio-oil was also confirmed through FTIR analysis using a Shimadzu IR Prestige-21.

The surface characteristics of biochar derived from both catalytic and non-catalytic processes were assessed employing SEM and TEM (JSM-5910 JEOL and JEM-2100 JEOL), respectively. For TEM investigation, the biochar was dissolved in acetone and then sonicated for five minutes. A drop of the sonicated colloidal solution was then placed onto a formvar-coated grid, allowed to air dry, and then transferred to the analytical chamber for examination.

3. Results and discussion

3.1. Raw biomass properties

The morphology and elemental analysis of raw *Citrus limetta* waste were studied using SEM-EDX. The SEM image is given in Fig. 2, which displays a highly porous structure. The disordered clusters with spongy holes are visible within the image. A thorough examination features closed-off microstructures, variable particle size distribution, and irregular and porous surfaces. The particles also varied in size and shape. The results are in conformity with some previous studies. Kamsonlian *et al.*[20] performed SEM analysis of orange peel and witnessed a porous surface with irregularly shaped pores of varying sizes. The surface morphology of lemon peel was also examined by Thirumavalavan *et al.*[21] using SEM, and they found a porous surface with a pore size of 39.483 Å.

Fig. 3 represents the elemental composition of raw *Citrus limetta* waste having mass percentage of carbon (61.99%), oxygen (33.32%), potassium (3.23%) and calcium (1.46%) respectively. The results coincide with previously reported studies. Kamsonlian *et al.*[20] conducted EDX analysis of orange peel and observed the following weight percentages of chemical compositions: 33.22% C, 44.12% O, 13.02% K, 1.12% Si, 0.4% Ca, 1.30% Na, 1.34% Al, and 3.30% Mg. According to Palaniappan *et al.*'s EDX study of sweet orange (*Citrus x sinensis*) fruit waste, the content of carbon and oxygen was the largest in the sample, which were 35.5% and 42.6%, respectively.[22]

3.2. Thermogravimetric analysis and kinetics

Thermogravimetry of citrus waste loaded with zeolite β, ammonium was conducted at a temperature programme rate of 15 °C min^{-1}, and the results are portrayed in the TG/DTG curve shown in
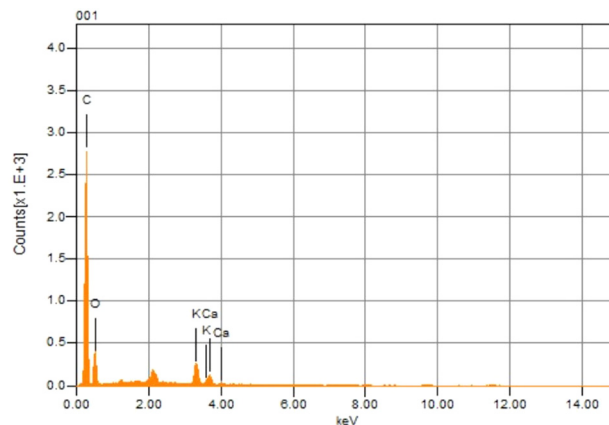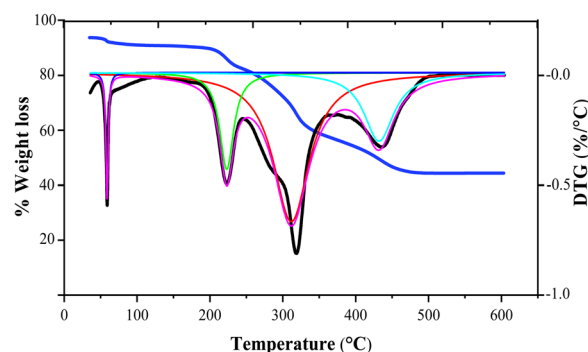

Fig. 3 EDX analysis of *Citrus limetta* waste.

Fig. 4 TG/DTG analysis of *Citrus limetta* waste in the presence of zeolite β, ammonium at a heating rate of 15 °C min^{-1}.

Fig. 4 and Table 1.[23] Utilizing the curve deconvolution method and application of Lorentzian peak function to the TG curve, it was determined that weight loss occurred in four distinct phases between room temperature and 600 °C, with no additional peak noted. The initial weight loss was attributed by the physical desorption of vapours at temperature below 100 °C. For hemicellulose, the T_{max} was determined to be 223 °C. In the case of cellulose degradation, the T_{max} was found to be 318 °C, while for lignin, it was observed at 436 °C. These findings align with earlier investigations. Nisar *et al.*[24] studied the pyrolysis of sugarcane bagasse with and without CuO. Their findings revealed a consistent four-step weight loss processes, which was attributed by the elimination of moisture and the breakdown of hemicellulose, cellulose, and lignin. Moreover, the findings of Pravin Kumar *et al.*[25] on banana peel pyrolysis are also in accord with this study.

The kinetic study thermal degradation experiments of citrus waste loaded with zeolite β, ammonium was conducted at

Table 1 Data obtained from TG/DTG analysis of *Citrus limetta* waste in the presence of zeolite β, ammonium at a heating rate of 15 °C min^{-1}

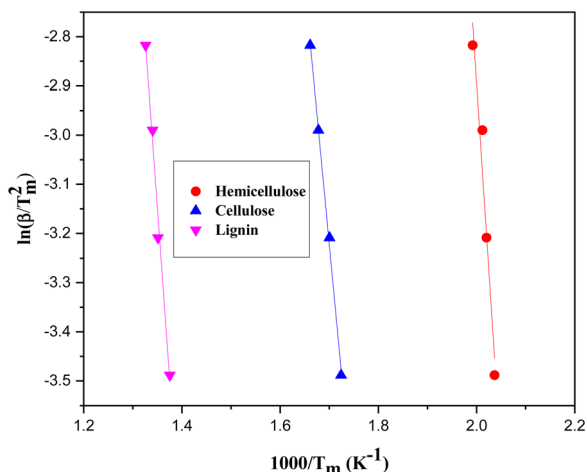| Temp/°C	T_{max}/°C	Component
179–280	223	Hemicellulose
280–391	318	Cellulose
391–527	436	Lignin

Fig. 5 Kissinger plots derived from the degradation of *Citrus limetta* waste loaded with zeolite β, ammonium.

temperature programme rate of 15, 20, 25, and 30 °C min⁻¹. The obtained data were used to determine E_a and A-factor applying Kissinger equation. The plots of $\ln \beta/T_m^2$ *vs.* $1000/T_m$ were constructed (Fig. 5), allowing for the extraction of E_a and A-factor from the resulting graphs. The calculated values (Table 2) showed that zeolite β, ammonium acted as a good catalyst for citrus waste decomposition, evidenced by the lower activation energies required for the decomposition of hemicellulose (83.14 kJ mol⁻¹), cellulose (108.08 kJ mol⁻¹) and lignin (124.71 kJ mol⁻¹) compared to non-catalytic reactions, which showed activation energies of 99.76, 157.96, and 174.59 kJ mol⁻¹, respectively.[7] This trend aligns with findings from other biomass pyrolysis studies. For example, in a study on the decomposition of peanut shells, the authors, calculated the E_a values (by Kissinger method) in the absence of the catalyst as 108.1, 116.4, and 182.9 kJ mol⁻¹ for hemicellulose, cellulose, and lignin, respectively. However, in the presence of the catalyst, the E_a values were found to be 66.5, 74.8, and 133 kJ mol⁻¹ for the same components, exhibiting termite hill as an efficient catalyst.[26] Varma *et al.*[27] used a thermogravimetric analyzer to conduct pyrolysis studies of peanut shells at heating rates of 10, 20, and 30 °C min⁻¹. The Kissinger equation was used to determine E_a and A-factor. The calculated average E_a was observed to be 109.05 kJ mol⁻¹. Similarly, in a study on sugarcane bagasse decomposition using Kissinger method,[24] a reduction in E_a values were noted for the catalyzed decomposition of hemicellulose, cellulose, and lignin *vis-a-vis* the uncatalyzed reaction. Lopez-Velazquez *et al.*[28] conducted pyrolysis of orange waste and calculated activation energies as 117, 105 and 260 kJ mol⁻¹ for the decomposition of hemicellulose, cellulose and lignin, respectively.

Table 2 Kinetic parameters calculated using the Kissinger method

Component	Parameters		
	E_a/kJ mol⁻¹	A/min⁻¹	R^2
Hemicellulose	83.14	6.3×10^4	0.979
Cellulose	108.082	9.4×10^6	0.939
Lignin	124.71	2.6×10^9	0.951

3.3. Optimization of experimental conditions for pyrolysis

Pyrolysis tests were carried out between 280 and 350 °C to evaluate how temperature affects the pyrolysis of citrus waste. The pyrolysis products from citrus wastes treated with zeolite β, ammonium at varying temperatures, catalyst concentrations and reaction times are shown in Fig. 6a, b and c, respectively. These figures depict the resulting bio-oil, char and gas yields, highlighting the influence of experimental conditions on the distribution of pyrolysates. Fig. 6a illustrates the effect of temperature on the catalytic degradation of citrus waste. The plot indicates that the production of liquid product increased gradually, peaking at 300 °C, before declining with a further increase in temperature. In contrast, the yield of gas fraction improved steadily as the temperature rose. These results demonstrate that the use of zeolite β, ammonium catalyst effectively lowered the temperature required for maximum bio-oil production from citrus waste, establishing 300 °C as the optimal temperature for oil production with this catalyst. This suggests that zeolite β, ammonium outperforms pumice, as reported in our previous investigation.[7] For comparison, Zhang *et al.*[29] examined that the optimum temperature for hydrothermal liquefaction of lemon peel was 336 °C, which is very close to our data. Additionally, Alvarez *et al.*[30] achieved a 54.6% (by weight) yield of bio-oil at 425 °C during the fast pyrolysis of citrus waste. Moreover, the figure demonstrates
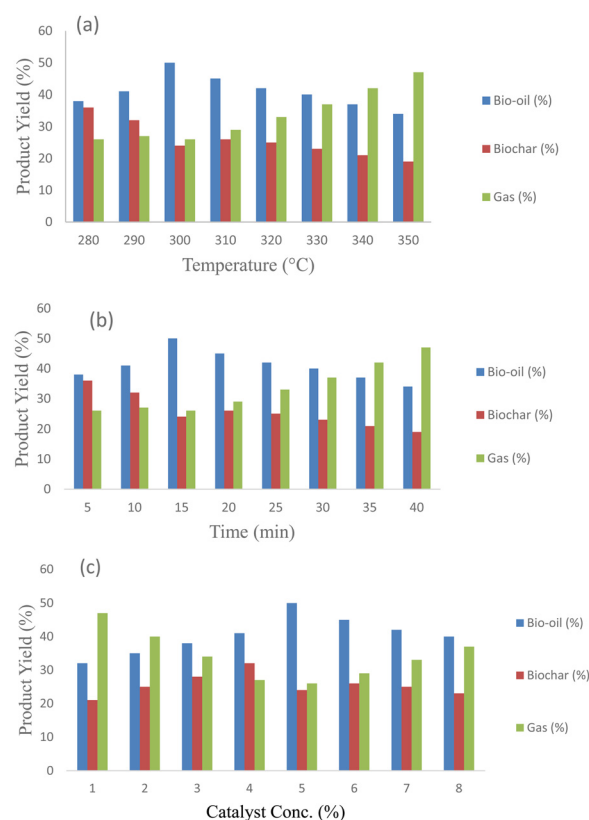

Fig. 6 Pyrolysis of *Citrus limetta* loaded with zeolite β, ammonium. (a) Temperature optimization, (b) time optimization, and (c) catalyst optimization.

Table 3 Pyrolysate yields from different biomasses under various conditions

| Biomass | Catalyst | Optimum temp./°C | Product yield/wt% | | | Ref. |
			Bio-oil	Gases	Bio-char	
Grapefruit waste	Nickel oxide	420	33	35	32	19
Almond shells	Zinc oxide	420	40	10	50	18
Cotton seed press cake	Nickel doped zeolite Y, hydrogen	300	35	17	48	36
Pomegranate peels	Sulfonated tea waste	330	56	6	37	9
Citrus limetta waste	Pumice	320	45	20	35	7
Citrus limetta waste	Zeolite β, ammonium	300	50	26	24	This work

that as the temperature increases, the gaseous fraction rises while that of the bio-oil shrinks, which is attributed to the secondary degradation of bio-oil.[31] Miranda *et al.*[32] conducted bench-scale pyrolysis experiments of citrus waste and observed that increasing pyrolysis temperature resulted in decreased char yield and increasing volatile content. Another primary objective of this work was to find out the optimal time at optimum temperature for pyrolyzing citrus waste. Fig. 6b illustrates the time optimization of the pyrolysis reaction. The maximum oil was produced at a time of 15 minutes, beyond which the production of bio-oil decreased. It also indicates that an increase in residence time led to a higher gaseous yield, while the biochar yield decreased with prolonged time. These findings align closely with a previous study on the degradation of sesame biomass.[33]

To determine the impact of zeolite β, ammonium concentration on the pyrolysates yield, the sample was mixed with varying percentages of zeolite β, ammonium (1%, 3%, 5%, 7%, and 9%) at optimal temperature and time. The results are given in Fig. 6c. When the catalyst was combined with the sample up to 5%, maximum bio-oil was obtained. Beyond that concentration, it has a negative effect. This is because raising the concentration of the catalyst causes liquefaction increase, but it also has an adverse effect above the ideal threshold of 5%. Additionally, catalyst poisoning is caused by the adsorption of bio-oil molecules on the catalysts' high specific surface area. This trend is in line with several previous works. Samolada

et al.[34] studied the pyrolysis of lignocellulose and discovered that enhancing the zeolite content lowered the amount of bio-oil while increasing the amount of gases. Through the pyrolysis of citrus waste, Poddar *et al.*[35] showed that the action of ZnO enhanced the bio-oil output (49.39 wt%) as compared to non-catalytic ones (30.75 wt%). Furthermore, gas production was found to increase with an increase in temperature.

A comparison of oil yield in this work with previous studies is presented in Table 3. It is clear from the data that sufficient quantity of bio-oil (50%) was produced from *Citrus limetta* waste in the presence of zeolite β, ammonium at a lower temperature of 300 °C.

3.4. Characterization of pyrolysates

3.4.1. GC-MS Analysis of bio-oil. A GC-MS machine was employed to chemically characterize the produced bio-oil, and the chromatogram is depicted in Fig. 7. A detailed summary of the identified products, including their molecular formula, name, molecular weight, percent area, and retention time, is provided in Table 4. The current findings indicate that catalytic pyrolysis greatly enhanced both the quantity and diversity of oil components produced compared to our previous study.[26] Notably, when comparing the catalytic bio-oil derived from citrus waste with the non-catalytic bio-oil,[7] it was noted that the bio-oil produced with zeolite β, ammonium contained certain fuel range components, such as phenol and benzene derivatives.
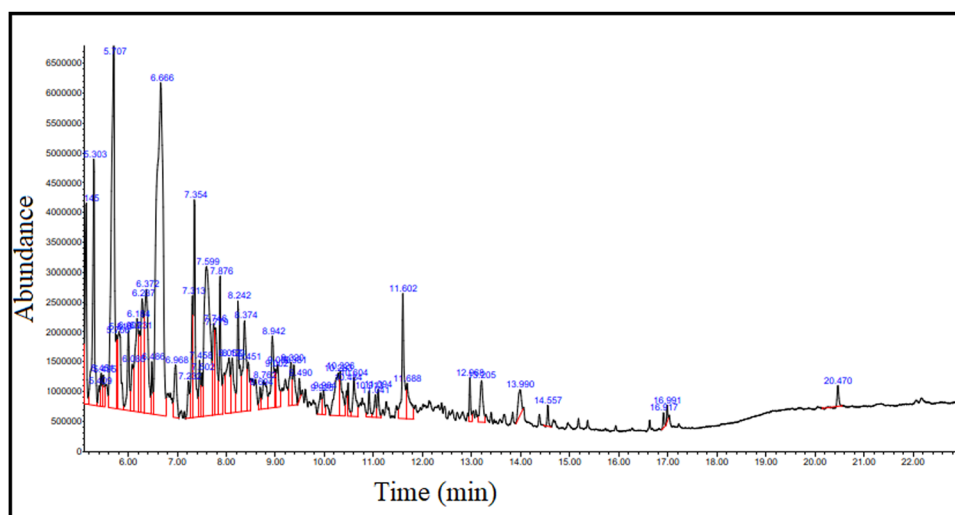

Fig. 7 GC-MS chromatogram of bio-oil produced by the thermo-catalytic decomposition of *Citrus limetta* waste.

Table 4 GC-MS profiling of chemical compounds in bio-oil produced by the thermo-catalytic decomposition of *Citrus limetta* waste

S. no.	*R*/*T* (min)	Component	Chemical formula	Molecular weight	Area %
1	5.14	Maltol	$C_6H_6O_3$	126.11	2.81
2	5.30	Hydrazine, 3 fluorophenyl	$C_6H_7FN_2$	126.13	4.18
3	5.41	Triethylenediamine	$C_6H_{12}N_2$	112.17	0.23
4	5.45	Furan, 4-methyl-2-propyl	$C_8H_{12}O$	124.18	0.44
5	5.49	2(1*H*)-Pyridinone	C_5H_5NO	95.09	0.49
6	5.71	4*H*-Pyran-4-one,2,3-dihydro-3,5-dihydroxy-6-methyl	$C_6H_8O_4$	144.12	9.68
7	5.77	4(1*H*)-Pyridone	C_5H_5NO	95.09	0.79
8	5.81	3-Pyridinol	C_5H_5NO	95.09	2.24
9	6.01	Phenol, 3-amino	C_6H_7NO	109.12	1.36
10	6.09	2(3*H*)-Furanone, dihydro-5-pentyl	$C_9H_{16}O$	156.22	0.79
11	6.18	2(3*H*)-Furanone, 5-butyldihydro	$C_8H_{14}O_2$	142.19	2.72
12	6.23	2-Hydroxy-5,5-dimethyl-hex-2-en-4-one	$C_8H_{14}O_2$	142.20	1.04
13	6.29	Furan, 2-ethoxy-2,3-dihydro-4-methyl	$C_7H_{12}O_2$	128.17	2.41
14	6.37	2-Pentene, 1-(pentyloxy)-, (*E*)-(*E*)-1-Pentyloxy-2-pentene	$C_{10}H_{20}O$	156.26	4.05
15	6.49	2-Hydroxy-3-propyl-2-cyclopenten-1-one	$C_8H_{12}O_2$	140.17	0.62
16	6.67	Phenol, 2-ethoxy	$C_8H_{10}O_2$	138.16	17.79
17	6.97	2,5-Dimethyl-4-hydroxy-3(2*H*)-furanone	$C_6H_8O_3$	128.13	1.21
18	7.23	*meta*-Methoxybenzenethiol	C_7H_8OS	140.20	0.57
19	7.31	1,2-Benzenediol,3-methyl	C_7H_8O	124.13	1.68
20	7.35	1,4-Benzenediol, 2,3,5-trimethyl	$C_9H_{12}O_2$	152.19	3.30
21	7.46	Phenol, 4-ethyl-2-methoxy-	C_9H_{12}	152.19	0.74
22	7.50	Creosol	$C_8H_{10}O_2$	138.16	0.50
23	7.59	6-Methyl-3(2*H*)-pyridazinone	$C_5H_6N_2O$	110.11	7.32
24	7.75	Benzoic acid, 2,3-dihydroxy	$C_7H_6O_4$	154.12	1.43
25	7.78	1,2-Benzenediol, 4-methyl	C_7H_8O	124.13	1.87
26	7.88	2-Methoxy-4-vinylphenol	$C_9H_{10}O_2$	150.22	1.95
27	8.06	2,5-Diethylphenol	$C_{10}H_{14}O$	150.22	1.79
28	8.12	3-Thiophenecarboxylic acid	$C_5H_4O_2S$	128.15	1.44
29	8.24	Phenol, 2,6-dimethoxy-	$C_8H_{10}O_3$	154.16	2.11
30	8.37	1,4-Benzenediol, 2-methyl-	$C_7H_8O_2$	124.13	2.54
31	8.45	2-Ethyl-4,6-dimethyltetrahydropyran	$C_9H_{18}O$	142.24	0.78
32	8.69	2,5-Dihydroxypropiophenone	$C_9H_{10}O_3$	166.17	0.30
33	8.76	3-Cyclohexen-1-one,2-isopropyl-5-methyl	$C_{10}H_{16}O$	152.23	0.99
34	8.94	Benzene, 2-fluoro-1,3,5-trimethyl-	$C_9H_{11}F$	138.18	1.65
35	9.01	Acetic acid, heptyl ester	$C_9H_{18}O_2$	158.23	0.52
36	9.05	4-Hydroxy-5,6-epoxy-beta-ionone	$C_{13}H_{20}O_3$	224.30	0.91
38	9.38	Phenol, 2-methoxy-3-methyl ester	$C_8H_{10}O_2$	138.16	0.82
39	9.49	2,4,6-Octatriene, 2,6-dimethyl-	$C_{10}H_{16}$	136.23	0.24
40	9.92	Benzene, 4-ethyl-1,2-dimethoxy	$C_{10}H_{14}O_2$	166.21	0.43
41	9.98	Tricyclo[3.3.2.0(3,7)]decan-9-one	$C_{10}H_{14}O$	150.22	0.42
42	10.28	1,3-Oxathiolane,2-(4 chlorophenyl)-2-methyl	$C_{10}H_{11}ClOS$	214.71	1.62
43	10.33	3-Hydroxy-4-methoxybenzoic acid, methyl ester	$C_9H_{10}O_4$	182.17	1.12
44	10.48	5-*tert*-Butylpyrogallol	$C_{10}H_{14}O_3$	182.22	0.41
45	10.60	Cyclopropane,1-ethoxy-2,2-dimethyl-3-(2 phenylethenylidene)	$C_{15}H_{18}O$	214.31	0.97
46	10.91	3*H*-Benz[*e*]indene, 2-methyl	$C_{14}H_{12}$	180.24	0.41
47	11.04	Anthracene, tetradecahydro	$C_{14}H_{24}$	192.34	0.35
48	11.09	Carbamic acid, methylphenyl-, ethyl ester	$C_{10}H_{13}NO_2$	179.22	0.45
49	11.60	3,4-Dichlorobenzenethiol	$C_6H_3SHCl_2$	179.07	2.33
50	11.69	Hydrazine, (2,4-dichlorophenyl)	$C_6H_6Cl_2N_2$	177.03	1.16
51	12.97	Ethyl,4-hydroxy-3-methoxyphenylacetate	$C_{11}H_{14}O_4$	210.23	0.51
52	13.20	2,4-Imidazolidinedione,5-(4-hydroxyphenyl)	$C_9H_8N_2O_3$	192.17	1.06
53	13.99	beta.-(4-Hydroxy-3-methoxyphenyl)propionic acid	$C_{10}H_{12}O_4$	196.19	0.69
54	14.56	5,10-Diethoxy-2,3,7,8-tetrahydro-1*H*,6*H*-dipyrrolo[1,2-*a*:1′,2′*d*] pyrazine	$C_{14}H_{22}N_2O_2$	250.34	0.25
55	16.92	9,12-Octadecadienoic acid (*Z*,*Z*)	$C_{18}H_{32}O_2$	280.44	0.16
56	16.99	6-Octadecenoic acid	$C_{18}H_{34}O_2$	282.50	0.14
57	20.47	Dicyclohexyl phthalate	$C_{20}H_{26}O_4$	330.40	0.26

Additionally, the analysis revealed the presence of a variety of compounds such as furan, maltol, creosol, ester and oleic acid, suggesting that the bio-oil was upgraded and could serve as a promising candidate for biofuel. The results imply that zeolite β, ammonium played a crucial role in improving bio-oil quality by increasing the variety of compounds detected by GC/MS and expanding the spectrum of hydrocarbons present.

The results align with previous investigations in the field of catalytic pyrolysis. Bhoi *et al.*[37] explored the catalytic pyrolysis of biomass using zeolite-based catalysts designed to eliminate undesirable compounds and enhance the hydrocarbon yield in bio-oil. Similarly, Miranda *et al.*[32] utilized GC/MS to identify key components such as carboxylic acid, phenol, and aldehyde in the bio-oil produced by quickly pyrolyzing dry citrus peel. Significant compounds discovered were benzene, phenol, *n*-hexadecenoic acid, and 2-cyclopenten-1-one, 2-methyl. In another study, Qiao *et al.*[38] reported the presence of terpenic oxide, alcohols, esters, ketone, and aldehydes in the liquid
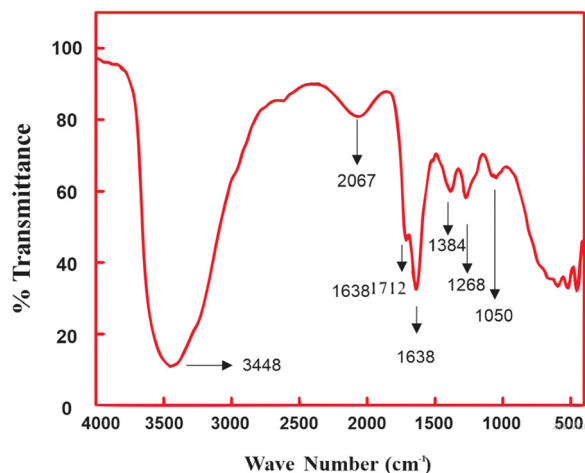
Fig. 8 FTIR spectrum of pyrolysis oil extracted from *Citrus limetta* waste.

Fig. 9 SEM images of *Citrus limetta* waste biochar: (a) without zeolite β, ammonium (b) with zeolite β, ammonium.

fraction obtained from citrus peels. Additionally, Kravetz *et al.*[39] discovered large peaks of 2-propanone, 1-hydroxy, 2-propenoic acid, succindialdehyde, furfural, 2-furanmethanol, 2(5H)-furanmethanol, and 3-methyl, 4-methyl-5H-furan-2-one in the bio-oil from Citrus sinensis waste.

3.4.2. FTIR of bio-oil. Fig. 8 shows the FTIR spectrum of bio-oil. For the alcohols and phenols that make up the major components of citrus peels, the strong peak (3448 cm^{-1}) is indicative of OH bond stretching, while the weak peak (1384 cm^{-1}) is due to OH bending. The C=C stretch can be seen by the peak at 2067 cm^{-1}. The C=O stretching of ketones, carboxylic acids, and esters is indicated by the absorbance peak at 1713 cm^{-1} and 1637 cm^{-1}. The peak at 1268 cm^{-1} due to C–O stretching vibrations points towards the existence of carboxylic acids, ethers, alcohols and esters. Aliphatic amines are indicated by the C–N stretching vibration at 1050 cm^{-1}. These outcomes from FTIR are in conformity with the study of Al-Layla *et al.*[40] on the pyrolysis of milk thistle waste.

In another study, lemon grass was flash-pyrolyzed by Madhu *et al.*[41] and FTIR was used to examine the produced bio-oil. The primary functional groups identified were associated with C=O stretching (carbonyls), C=O stretching (alcohols, ethers, carboxylic acids, and esters), C–N stretching (aliphatic amines)
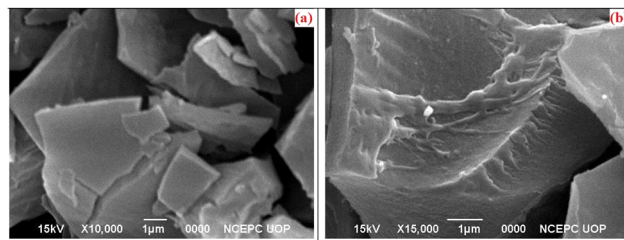
and OH (alcoholic and phenols). Likewise, Volpe *et al.*[42] utilized leftover orange and lemon peels to produce bio-oil. The functional groups they examined, according to FTIR analysis, were OH stretching (phenol), C=O stretching (ketone and carboxylic acids), and OH bending at 1370 cm^{-1}.

3.4.3. Fuel properties of the bio-oil. As indicated by the physicochemical characteristics, the bio-oil produced has a strong odor and is pale yellow in color. Other characteristics (Table 5) of the tested bio-oil, including density, viscosity and pH, were quite similar to those of bio-oils testified in previous research.[43,44]

3.4.4. Characterization of biochar. Fig. 9a and b display the SEM images of non-catalytic and catalytic biochar, respectively. The biochar obtained from non-catalytic decomposition (Fig. 9a) reveals a smooth disc-like texture, while catalytic biochar (Fig. 9b) exhibits an uneven and rough surface, which makes it suitable for many applications, for example, as adsorbent, energy storage supercapacitor, and catalyst.[53] These characteristics in biochar can be achieved through the pyrolysis of citrus wastes using a selected catalyst. The interaction between the catalyst and citrus wastes resulted in the formation of lumps-like structures in catalytic biochar, which possessed a larger surface area. The use of a catalyst induced significant morphological changes, causing surface deformation with highly developed pore structure, as also observed by many authors. Wang *et al.*[54] studied biochar produced after pyrolysis and observed irregular distributed pores on its surface, which broke and collapsed. Ali *et al.*[55] performed SEM analysis on both non-catalytic and catalytic biochar samples. They observed flat disc-like surface of non-catalyzed biochar as compared to catalytic biochar, which had an uneven, irregular and porous structure.

Table 5 Comparison of the physicochemical properties of bio-oil obtained from *Citrus limetta* waste with bio-oil from different sources

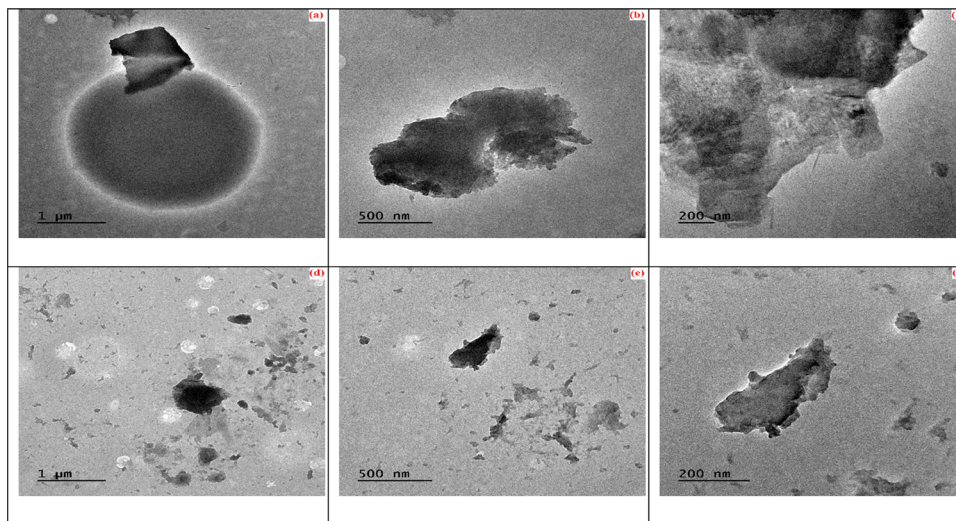| Biomass/catalyst	Density (kgm^{-3})	Viscosity (Pa.s)	pH	Ref.
Rice husk	1190	0.150	2.80	45
Pine wood (at 425 °C)	1174 ± 40	—	2.1 ± 0.09	46
Miscanthus	1050	—	2.95	47
Corn stover	1250	—	2.87	
Wood pellets	1230	—	2.80	
Cotton stalk	1160	0.140	—	48
Areca nut husk	980	0.078	—	43
Areca nut husk/ZSM-5	812	0.029	—	43
Cow hooves	1030 ± 100	0.010	—	49
Sugarcane bagasse	1211	0.004	—	50
Palm shell	1051	0.003	—	51
Pinewood waste	1140	0.001	—	52
Corn stalk	1220	0.168	3.20	44
Sweet lemon waste (at 300 °C)	980	0.168	3.5	This work

Fig. 10 TEM images of *Citrus limetta* waste biochar obtained at different magnifications: (a–c) without zeolite β, ammonium (d–f) with zeolite β, ammonium.

Transmission electron microscopy was employed to study the microstructure of *Citrus limetta* waste biochar. Fig. 10(a–c) presents the TEM images of non-catalytic biochar. The TEM images of non-catalytic biochar revealed a fused carbon skeleton, resulting in a compact structure with a small, rigid and even surface. In contrast, the biochar obtained from the catalytic process exhibited a different morphology, as exhibited in Fig. 10(d–f). The TEM images show an increase in the surface pore size, resulting from the agglomeration of carbon particles. This agglomeration process captured carbon molecules, imparting various rubber-like qualities to the biochar. The acquired data is in agreement with the findings reported in existing literature. Ali *et al.*[55] performed the TEM analysis of both un-catalyzed and catalyzed biochar samples. They observed that bare biochar exhibited a small particle size and displayed a highly rigid structure. In contrast, catalytic biochar showed an irregular surface and large pore size, obtained as a result of agglomeration of carbon particles. Li *et al.*[56] carried out TEM analysis of biochar and revealed the accumulation of similar carbon particles, which were equally distributed in the carbon matrix.

4. Conclusions

Our research centered on utilizing zeolite β, ammonium as a catalyst for pyrolysis to transform waste citrus materials into valuable products while also figuring out the reaction's kinetic parameters. Thermogravimetric analysis was conducted on citrus waste in an inert atmosphere over zeolite β, ammonium at various heating rates. Using Kissinger method, the E_a for hemicelluloses, cellulose, and lignin was determined as 83.14, 108.082, and 124.71 kJ mol^{-1}, respectively. Moreover, for bio-oil production, pyrolysis was done in a particular salt bath in a nitrogen environment at 280–350 °C in the presence of zeolite β, ammonium catalyst. The pyrolyzed oil obtained under the optimized conditions was characterized using GC-MS, and it was found that some additional fuel range hydrocarbons were present, as compared to non-catalyzed reaction. The existence of phenols and alcohols, the primary constituents of citrus peel, was further verified by FTIR spectrum data. Furthermore, additional bending-oriented and stretching-supporting peaks verified the occurrence of carboxylic, ether, alcoholic, esters, and aliphatic amine groups. In general, the findings of this investigation indicated that the use of zeolite β, ammonium not only improved the quality of oil but also reduced the temperature and E_a of the pyrolysis reaction. The work reported herein reveals that citrus waste in the presence of zeolite β, ammonium catalyst has enormous potential for use in the production of biofuel. It can also be argued that with appropriate upgradation, the oil produced by citrus waste could be utilized as an alternative biofuel.

Author contributions

Faisal Muhammad., investigation, methodology, writing – original draft. Jan Nisar., conceptualization, funding acquisition, resources, project administration. Ghulam Ali., writing, results and analysis. Farooq Anwar., review and editing. Wan Azlina Wan Abdul Karim Ghani., review and editing and visualization. Ahsan Sharif., editing and visualization. Ejaz Ahmed., editing and visualization.

Nomenclature and abbreviations

E_a	Activation energy
A	Frequency factor
$β$	Temperature programmed rate
T_m	Temperature maximum degradation
R	Gas constant
GCMS	Gas chromatography–mass spectrometry

FTIR Fourier transform infrared spectroscopy
TGA   Thermogravimetric analysis
SEM   Scanning electron microscopy
TEM   Transmission electron microscopy

Data availability

The authors declare that the data are available in the manuscript in the form of tables and figures.

Conflicts of interest

The authors have no conflicts of interest to declare.

Acknowledgements

References

1 R. Avtar, et al., Population–urbanization–energy nexus: a review, Resources, 2019, 8(3), 136.

2 F. Akram, et al., Current trends in biodiesel production technologies and future progressions: A possible displacement of the petro-diesel, J. Cleaner Prod., 2022, 133479.

3 M. Al Rashdan, M. Al Zubi and M. Al Okour, Effect of using new technology vehicles on the World's environment and petroleum resources, J. Ecol. Eng., 2019, 20, 1.

4 M. Afraz, et al., Production of value added products from biomass waste by pyrolysis: An updated review, Waste Manag. Bull., 2024, 1(4), 30–40.

5 J. Nisar, et al., Production of Bio-Oil from De-Oiled Karanja (Pongamia pinnata L.) Seed Press Cake Via Pyrolysis: Kinetics and Evaluation of Anthill as the Catalyst, Sustainable Chem., 2022, 3(3), 345–359.

6 W. Ahmad, J. Nisar, F. Anwar and F. Muhammad, Future prospects of biomass waste as renewable source of energy in Pakistan: A mini review, Bioresour. Technol. Rep., 2023, 101658.

7 F. Muhammad, et al., Improved bio-oil yield from thermocatalytic pyrolysis of Citrus limetta waste over pumice: Determination of kinetic parameters using Kissinger method, Bioresour. Technol. Rep., 2023, 24, 101635.

8 M. Amin, et al., Hydrogen production through renewable and non-renewable energy processes and their impact on climate change, Int. J. Hydrogen Energy, 2022, 47(77), 33112–33134.

9 N. U. Rehman, et al., Production of bio-oil from thermocatalytic decomposition of pomegranate peels over a sulfonated tea waste heterogeneous catalyst: a kinetic investigation, Energies, 2023, 16(4), 1908.

10 J. Nisar, et al., Thermo-catalytic decomposition of walnut shells waste over cobalt doped cerium oxide: Impact of catalyst on kinetic parameters and composition of bio-oil, Chem. Eng. Sci., 2023, 282, 119355.

11 S. F. Ahmed, et al., Utilization of nanomaterials in accelerating the production process of sustainable biofuels, Sustainable Energy Technol. Assess., 2023, 55, 102894.

12 S. Choudhary et al., in Pulses Waste to Biofuels, Agroindustrial Waste for Green Fuel Application, Springer, 2023, pp. 1–26.

13 W. Miao, et al., Biochar application enhanced rice biomass production and lodging resistance via promoting co-deposition of silica with hemicellulose and lignin, Sci. Total Environ., 2023, 855, 158818.

14 Y. Liu, E. Heying and S. A. Tanumihardjo, History, global distribution, and nutritional importance of citrus fruits, Compr. Rev. Food Sci. Food Saf., 2012, 11(6), 530–545.

15 D. Kundu et al., in Citrus fruits, Valorization of Fruit Processing By-products, Elsevier, 2020, 145–166.

16 A. Selvarajoo, et al., Biochar production via pyrolysis of citrus peel fruit waste as a potential usage as solid biofuel, Chemosphere, 2022, 133671.

17 R. L. Blaine and H. E. Kissinger, Homer Kissinger and the Kissinger equation, Thermochim. Acta, 2012, 540, 1–6.

18 J. Nisar, et al., Pyrolysis of almond shells waste: effect of zinc oxide on kinetics and product distribution, Biomass Convers. Biorefin., 2022, 12(7), 2583–2595.

19 J. Nisar, et al., Pyrolysis of juice-squeezed grapefruit waste: Effect of nickel oxide on kinetics and bio-oil yield, Int. J. Environ. Sci. Technol., 2022, 19(10), 10211–10222.

20 S. Kamsonlian, et al., Characterization of banana and orange peels: biosorption mechanism, Int. J. Sci. Technol. Manage., 2011, 2(4), 1–7.

21 M. Thirumavalavan, et al., Cellulose-based native and surface modified fruit peels for the adsorption of heavy metal ions from aqueous solution: Langmuir adsorption isotherms, J. Chem. Eng. Data, 2010, 55(3), 1186–1192.

22 M. Palaniappan, et al., Synthesis and suitability characterization of microcrystalline cellulose from Citrus x sinensis sweet orange peel fruit waste-based biomass for polymer composite applications, J. Polym. Res., 2024, 31(4), 105.

23 R. Torres-Sciancalepore, et al., Two-step valorization of invasive species Rosa rubiginosa L. husk waste through eco-friendly optimized pectin extraction and subsequent pyrolysis, J. Environ. Chem. Eng., 2023, 11(5), 110802.

24 J. Nisar, et al., Kinetics of pyrolysis of sugarcane bagasse: effect of catalyst on activation energy and yield of pyrolysis products, Cellulose, 2021, 28, 7593–7607.

25 S. A. Pravin Kumar, et al., Thermogravimetric study and kinetics of banana peel pyrolysis: a comparison of 'model-free' methods, Biofuels, 2022, 13(2), 129–138.

26 J. Nisar, et al., Enhanced Bio-Oil Yield from Thermal Decomposition of Peanut Shells Using Termite Hill as the Catalyst, Energies, 2022, 15(5), 1891.

27 A. K. Varma, et al., Investigation of kinetic and thermodynamic parameters for pyrolysis of peanut shell using thermogravimetric analysis, Biomass Convers. Biorefin., 2020, 1–12.

28 M. Lopez-Velazquez, et al., Pyrolysis of orange waste: a thermo-kinetic study, J. Anal. Appl. Pyrolysis, 2013, 99, 170–177.

29 B. Zhang, et al., Hydrothermal liquefaction of fresh lemon-peel: parameter optimisation and product chemistry, Renewable Energy, 2019, 143, 512–519.

30 J. Alvarez, et al., Valorization of citrus wastes by fast pyrolysis in a conical spouted bed reactor, Fuel, 2018, 224, 111–120.

31 R. J. Westerhof, et al., Effect of temperature in fluidized bed fast pyrolysis of biomass: oil quality assessment in test units, Ind. Eng. Chem. Res., 2010, 49(3), 1160–1168.

32 R. Miranda, et al., Pyrolysis of sweet orange (Citrus sinensis) dry peel, J. Anal. Appl. Pyrolysis, 2009, 86(2), 245–251.

33 J. Nisar, et al., Kinetics of the pyrolysis of cobalt-impregnated sesame stalk biomass, Biomass Convers. Biorefin., 2020, 10, 1179–1187.

34 M. Samolada, A. Papafotica and I. Vasalos, Catalyst evaluation for catalytic biomass pyrolysis, Energy Fuels, 2000, 14(6), 1161–1167.

35 S. Poddar, J. Ullas Krishnan and J. S. Chandra Babu, Non-catalytic and catalytic pyrolysis of citrus waste (orange peel), Indian Chem. Eng., 2022, 1–28.

36 M. Afraz, et al., Thermo-catalytic decomposition of cotton seed press cake over nickel doped zeolite Y, hydrogen: enhanced yield of bio-oil with highly selective fuel-range hydrocarbons, RSC Adv., 2024, 14(43), 31549–31559.

37 P. Bhoi, et al., Recent advances on catalysts for improving hydrocarbon compounds in bio-oil of biomass catalytic pyrolysis, Renewable Sustainable Energy Rev., 2020, 121, 109676.

38 Y. Qiao, et al., Characterization of aroma active compounds in fruit juice and peel oil of Jinchen sweet orange fruit (Citrus sinensis (L.) Osbeck) by GC-MS and GC-O, Molecules, 2008, 13(6), 1333–1344.

39 C. Kravetz, et al., Characterization of selected pyrolysis products of diseased orange wood, BioResources, 2020, 15(3), 7118–7126.

40 N. M. Al-Layla, L. A. Saleh and A. B. Fadhil, Liquid bio-fuels and carbon adsorbents production via pyrolysis of non-edible feedstock, J. Anal. Appl. Pyrolysis, 2021, 156, 105088.

41 P. Madhu, T. S. Livingston and H. Kanagasabapathy, Flash pyrolysis of lemon grass (Cymbopogon flexuosus) for bio-oil production in an electrically heated fluidized bed reactor, Waste Biomass Valorization, 2018, 9, 1037–1046.

42 M. Volpe, et al., Upgrade of citrus waste as a biofuel via slow pyrolysis, J. Anal. Appl. Pyrolysis, 2015, 115, 66–76.

43 R. K. Mishra, et al., Thermocatalytic Pyrolysis of Waste Areca Nut into Renewable Fuel and Value-Added Chemicals, ACS Omega, 2024, 9, 25779–25792.

44 M. H. Duku, Bio-oil production from Lignocellulosic biomass using fast pyrolysis in a fluidized-bed reactor. 2015.

45 Z. Ji-Lu, Bio-oil from fast pyrolysis of rice husk: Yields and related properties and improvement of the pyrolysis system, J. Anal. Appl. Pyrolysis, 2007, 80(1), 30–35.

46 S. Thangalazhy-Gopakumar, et al., Physiochemical properties of bio-oil produced at various temperatures from pine wood using an auger reactor, Bioresour. Technol., 2010, 101(21), 8389–8395.

47 S. Hosseinnezhad, et al., Physiochemical characterization of synthetic bio-oils produced from bio-mass: a sustainable source for construction bio-adhesives, RSC Adv., 2015, 5(92), 75519–75527.

48 J.-l Zheng, W.-m Yi and N.-n Wang, Bio-oil production from cotton stalk, Energy Convers. Manage., 2008, 49(6), 1724–1730.

49 J. Chukwuneke, et al., Production and physico-chemical characteristics of pyrolyzed bio-oil derived from cow hooves, Arab J. Basic Appl. Sci., 2022, 29(1), 363–371.

50 M. Garcìa-Pèrez, A. Chaala and C. Roy, Vacuum pyrolysis of sugarcane bagasse, J. Anal. Appl. Pyrolysis, 2002, 65(2), 111–136.

51 F. Abnisa, et al., Utilization possibilities of palm shell as a source of biomass energy in Malaysia by producing bio-oil in pyrolysis process, Biomass Bioenergy, 2011, 35(5), 1863–1872.

52 M. Amutio, et al., Influence of temperature on biomass pyrolysis in a conical spouted bed reactor, Resour., Conserv. Recycl., 2012, 59, 23–31.

53 S. Xiu, A. Shahbazi and R. Li, Characterization, modification and application of biochar for energy storage and catalysis: a review, Trends Renewable Energy, 2017, 3(1), 86–101.

54 W. Wang, et al., Effect of nickel salts on the production of biochar derived from alkali lignin: properties and applications, Bioresour. Technol., 2021, 341, 125876.

55 G. Ali, et al., Production of Fuel Range Hydrocarbons from Pyrolysis of Lignin over Zeolite Y, Hydrogen, Energies, 2023, 16(1), 215.

56 C. Li, et al., Impact of heating rates on the evolution of function groups of the biochar from lignin pyrolysis, J. Anal. Appl. Pyrolysis, 2021, 155, 105031.